

Controlling excess noise in fiber-optics continuous-variable quantum key distribution

Jérôme Lodewyck,^{1,2} Thierry Debuisschert,¹ Rosa Tualle-Brouri,² and Philippe Grangier²

¹Thales Research and Technologies, RD 128 91767 Palaiseau CEDEX France

²Laboratoire Charles Fabry de l'Institut d'Optique, Campus Universitaire, Bâtiment 503 91403 Orsay CEDEX France

(Received 13 July 2005; published 22 November 2005)

We describe a continuous-variable coherent-states quantum-key distribution system working at 1550 nm, and entirely made of standard fiber optics and telecommunications components, such as integrated-optics modulators, couplers and fast InGaAs photodiodes. The setup is composed of an emitter randomly modulating a coherent state in the complex plane with a doubly Gaussian distribution, and a receiver based on a shot-noise limited time-resolved homodyne detector. By using a reverse reconciliation protocol, the device can transfer a raw key rate up to 1 Mbit/s, with a proven security against Gaussian or non-Gaussian attacks. The dependence of the secret information rate of the present fiber setup is studied as a function of the line transmission and excess noise.

DOI: [10.1103/PhysRevA.72.050303](https://doi.org/10.1103/PhysRevA.72.050303)

PACS number(s): 03.67.Dd, 42.50.Lc, 42.81.-i

Quantum-key distribution (QKD) is a cryptographic process enabling two distant actors—Alice and Bob—to share a common secret key, unknown to a potential eavesdropper—Eve. Quantum laws enable Alice and Bob to detect Eve, and to quantify the amount of information she acquired about the key, thus allowing unconditionally secure information transfer. For this purpose Alice and Bob must choose a proper encoding of information using noncommuting quantum channel variables. These variables are generally the polarization or phase of single photon pulses, requiring specifically developed components such as single photon sources and photon counters.

In contrast, continuous-variable QKD schemes typically use quadrature amplitude of light beams as information carriers, and homodyne detection rather than photon counting. For instance, a QKD scheme based on encoding information in the phase and amplitude of bright coherent states [1] has been recently demonstrated using a table-top setup at 780 nm [2]. This scheme, which we are also using here, is based upon the idea of “reverse reconciliation” [3] to extract secret information from the data provided by homodyne detection. In several recent articles, this protocol, which we will denote as the reverse reconciled coherent state (RRCS), has been proven able to transmit secret keys for arbitrary channel transmission, and to be secure against non-Gaussian [4] and collective [5,6] attacks.

The security proof of RRCS presented in [4], makes use of entropic Heisenberg inequalities to set an upper bound on Eve and Bob’s Shannon mutual information I_{BE} about the key. This bound is computable from the transmission signal-to-noise ratio (SNR). A secret key can possibly be extracted by error correction and privacy amplification based on Bob’s copy of the key if

$$\Delta I = I_{AB} - I_{BE} > 0.$$

This inequality can be satisfied in principle for any channel transmission, as it is also the case for photon-counting QKD. This means that vacuum noise, which is the continuous-variable equivalent to the photon losses encountered in photon-counting quantum cryptography, does not limit by

itself the range of QKD. The real limitation comes from errors in photon counting QKD [7], and it is associated with *excess noise* in the case of continuous variables. By definition, excess noise is the noise *above* the vacuum noise level associated with channel losses, and it is a major issue in continuous-variable QKD, as pointed out in various recent papers [3,8].

In particular, it has been shown in [3] that when the excess noise (referred to the channel input) reaches two times the shot-noise level, Eve can perform an intercept-resend attack on the channel and thus no secure key can be transmitted. As another illustration of the importance of excess noise, it has been pointed out in [9] that the presence of excess noise severely weakens protocols that use postselection to extract bits from the correlated Gaussian distributions shared by Alice and Bob [10,11].

A specific feature of the RRCS protocol is to use full Gaussian distributions for data transmission between Alice and Bob, enforcing that the optimal attack by Eve is also Gaussian [4]. In case Eve would like to try a less efficient non-Gaussian attack, the distribution received by Bob may not be Gaussian anymore, but the information acquired by Eve remains bounded by the variance of the noise measured by Alice and Bob. This is a very convenient feature, which requires us, however, to extract very efficiently the bits from the correlated Gaussian data. The combination of these features—Gaussian modulation and the resulting possibility to evaluate analytically the tolerance to excess noise—warrants that the secret bit rate can be evaluated simply from real transmission data.

It is also worth noticing that the use of quadrature modulation and homodyne detection in the RRCS protocol is well suited for telecommunications application, because it can be implemented with off-the-shelves fast and efficient telecommunications components, and use existing single mode telecommunications fibers. For this reason, it features a very high nominal secret key rate. As it will be discussed below, the target distance range for this kind of setup is several tens of kilometers, limited by the efficiency of classical bit error correction algorithms.

In this paper, we describe an all-fiber-optics continuous-

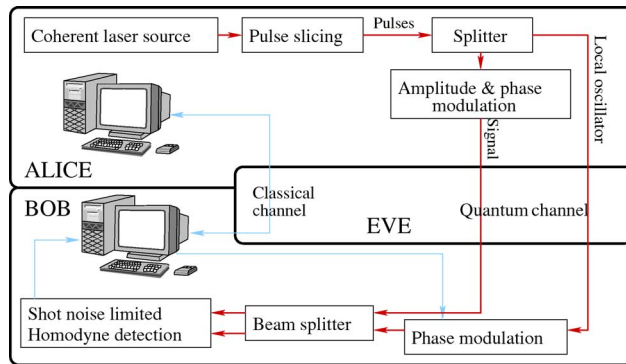


FIG. 1. (Color online) Experiment layout. Alice sends both modulated signal and phase reference to Bob. A random quadrature is measured by a time-resolved, shot-noise limited homodyne detection.

variable RRCS-QKD setup, and give an explicit evaluation of the available secret bit rate obtained by measuring the signal-to-noise degradation for various values of the line transmission, in the presence of technical excess noise. These results clearly show the importance of evaluating and controlling excess noise in continuous-variables QKD setups for a proper determination of the secret key rate.

The experimental scheme is composed of two independent modules. Alice, the sender, has to randomly displace coherent states in the complex Fresnel plane. Bob, the receiver, has to measure a random quadrature of the incoming signal, with a shot-noise limited pulsed homodyne detector (see Fig. 1).

Alice first generates 100-ns-wide pulses from a continuous-wave distributed feedback (DFB) laser diode emitting at 1550 nm with an integrated electro-optics modulator, driven by a pulse generator. These pulses are split into a strong phase reference (or local oscillator) of 10^8 photons per pulse, and a weak signal (typically 100 photons). Each signal pulse is a well-defined coherent quantum state of the light representing a channel symbol. To compensate for various losses in the phase reference optical path, the production of these pulses requires a laser power of about 100 mW at the diode output. Alice's setup is entirely made of polarization maintaining fibers in order to avoid polarization drifts at the modulators input, and relative polarization drifts between signal and local oscillator.

This signal is continuously modulated in phase and amplitude with computer-driven electro-optics amplitude and phase modulators, in order to place the coherent states in the complex plane. For our continuous-variable QKD protocol, the required modulation is a two-dimensional Gaussian distribution centered on zero, with a customizable variance. Due to modulators dynamics, the modulation is truncated to four standard deviations, thus resulting in an error of 0.3% on variances estimations. For a modulation variance of 40 photons per pulse, the modulation inaccuracy is typically less than 4% relative to the shot-noise variance, at rates up to 1 MHz. This 4% inaccuracy is equivalent to an excess noise (see below). It is mainly due to nonperfect static and dynamic modulator voltage settings, as well as large voltage rising times.

In the present implementation, the signal and phase reference are sent to Bob by using two separate fibers with a length of a few meters, properly isolated from external perturbations. In this configuration, we can simulate channel losses by varying Alice's modulation variance V_A . The reference level (which defines unity gain) is set to $V_A=40V_0$, where the shot-noise variance V_0 will be used as a reference for all noise levels in the following.

While this setup is suitable for our noise analysis, it is not optimized for field QKD, because over long distances two different single mode fibers will see large relative polarization and phase drifts. To get rid of these perturbations, the signal and local oscillator should be sent in the same fiber with a time delay. We have made preliminary tests for such a time multiplexing into a single fiber, using also an active polarization controller to avoid unwanted polarization drifts. The results are promising, but a full key distribution has yet to be performed in this configuration.

Bob's setup is composed of a shot-noise limited time-resolved homodyne detection. Weak signal pulses interfere with the phase reference, and light intensity in both output arms is measured with matched fast InGaAs photodiodes (10 GHz, 80% efficiency). The signal quadrature is then obtained by subtraction of the two photocurrents, amplified with a low noise charge amplifier [12] followed by a constant gain amplifying stage. Electronic noise from this amplification chain is 20 dB below the shot noise. A time-domain homodyne detection requires a precise balancing of the two arms with an accuracy better than 10^{-4} so that the residual unbalance does not saturate amplifiers. This is achieved with mechanical fiber-optics variable attenuators, which introduce small losses by bending the fiber. Such a balancing is very stable on time scales of several hours. Bob can select a desired quadrature at a 1-MHz rate with a phase modulator placed in the reference optical path. The present overall efficiency of the homodyne detector is about 60%. Photodiodes account for half of the losses, the remaining losses are due to fiber connectors. Other components (coupler, variable attenuator) have very low intrinsic insertion losses (typically 0.05 dB). To enhance the information rate, losses within the homodyne detection can be reduced by splicing fibers.

Alice and Bob are computer interfaced by a synchronous automatic data processing software. In order to fully implement a QKD scheme, we designed a communication protocol that can synchronize Alice and Bob and provide for channel parameters (gain, excess noise, and relative phase). The communication is split into independent blocks. The block size—typically 50000 pulses—is adjusted so that we can assume transmission parameters are constant over a block, while being large enough to make statistical tests. A block is composed of smaller (100 pulses long) structures, containing 80 useful modulation pulses and 20 test pulses (Fig. 2), forming a software detectable pattern. These test pulses consist of maximal amplitude and phase modulated coherent states. From these pulses, one can synchronize Alice and Bob, determine the mean signal, the relative phase between signal and local oscillator, and the phase and intensity noise. The properties of the test pulses are chosen so that all these parameters can be independently determined. By averaging test pulses over a block, we can get rid of the shot noise and

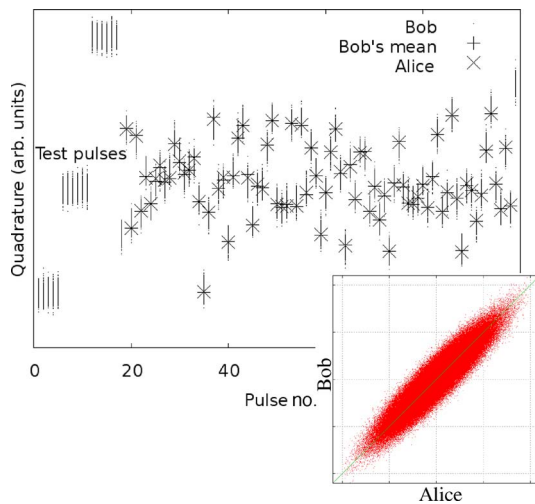


FIG. 2. (Color online) Random modulation. Alice’s random modulation is repeated every 100 pulses in order to observe the shot noise and modulation imperfections. The points are Bob’s measurement, × crosses are Alice’s modulation, and + crosses are Bob’s measurement average. The difference between + and × crosses represents the technical noise due to modulation imperfections, typically 4% of the shot-noise variance V_0 for a modulation variance of $40V_0$. These 100 pulses contain 20 test pulses (left part) and 80 useful modulation pulses. With truly random modulation we obtain correlation between Alice and Bob (bottom right), the width of the data set showing the total noise level referred to the input.

obtain accurate channel parameters determination. We note that the test pulses might be used or manipulated by the eavesdropper, and therefore all calibrations must also be doublechecked by statistics over a randomly chosen revealed sample from the Gaussian data set.

The setup described so far produces correlated Gaussian-distributed continuous variables at a 1-MHz rate. In order to evaluate the raw key rate from these correlations, we need to review noises sources appearing in the protocol (Fig. 3). As mentioned above, the decrease in SNR during propagation in the channel can be split into two different terms: the vacuum noise due to line losses, and the excess noise. In this picture, we can write the total added noise χ , referred to the input and expressed in shot-noise units, as $\chi = (1 - G)/G + \xi$, where G is the channel gain and ξ is the excess noise.

Even in the absence of Eve, excess noise is introduced by technical imperfection in our modulation system and by the laser diode phase noise. In principle, this excess noise is not due to Eve and could be considered unknown to her. However, the level of modulation and phase excess noise is drifting, depending on the modulators settings, and cannot be calibrated. Therefore, it is wiser to assume that it can be

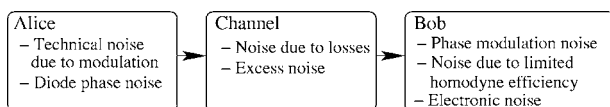


FIG. 3. Nature of noise sources found in the QKD device. Technical, phase, and electronic noises account for the total excess noise.

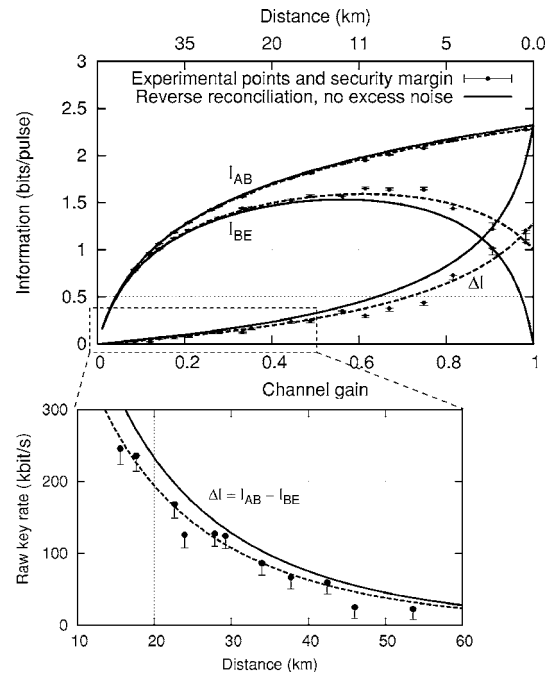


FIG. 4. Shannon mutual information per pulse shared by Alice and Bob. Solid lines define reverse reconciliation Shannon information rates for a lossy channel without excess noise. Because of technical noise, the experimental (dots) and theoretical (dashed lines) information rates achievable by the experiment are lower. The figure also shows security margins of $0.20V_0$ units on Bob’s output excess noise evaluation. The bottom left figure is a zoom of the advantage of Alice on Eve in terms of available information rate before binary processing. It is plotted as a function of the distance rather than the channel gain. It is equivalent to the secret key rate that would be obtained after applying perfect ($\beta=1$) error correction and privacy amplification to our data.

generated and controlled by Eve. Let us emphasize also that fiber optics without repeaters or amplifiers do not generally introduce excess noise. However, uncertainty on Bob’s estimation of the output noise is equivalent to an excess noise at the input, function of the line transmission, potentially accessible to Eve.

The phase noise level for maximum output intensity is typically $0.2V_0$, but it is as low as $0.1V_0$ when averaged over the Gaussian modulation. To achieve such a low phase noise, the laser diode must be strongly attenuated (≥ 80 dB) from its initial power of 100 mW, and the path difference between interferometer arms (a few tens of centimeters) has to be small compared to the laser coherence length. All in all, the total excess noise measured is $\xi=0.06V_0$ for a modulation variance $V_A=40V_0$, and decreases proportionally for lower variances.

Losses in Alice’s device do not matter since the reference level is calibrated at Alice’s output. Losses of the homodyne detector, while deteriorating Bob’s SNR, can be considered unrelated to Eve, and therefore do not contribute to her information. This approach, which considers Eve has no access to Bob’s hardware, is called a “realistic mode,” as opposed to a “paranoid mode” where Eve would be able to exploit internal defects of Bob’s setup. In any case, it is clear that the

homodyne detector efficiency η needs to be very carefully calibrated. In this realistic picture, we can derive mutual Shannon information rates as a function of the channel gain G and the excess noise ξ [2]

$$I_{AB} = \frac{1}{2} \log_2 \frac{\eta G V_A + 1 + \eta G \xi}{1 + \eta G \xi},$$

$$I_{BE}^{\max} = \frac{1}{2} \log_2 \frac{\eta G V_A + 1 + \eta G \xi}{\eta [1 - G + G \xi + G/(V_A + 1)] + 1 - \eta}.$$

All the quantities appearing in these formulas are measured by Alice and Bob. Experimental measurement of ξ for different channel transmissions enables to plot the rates I_{AB} and I_{BE} achieved by our setup as a function of G (Fig. 4). For this plot the homodyne efficiency η is 0.6, the modulation variance V_A is set to $40V_0$, and the excess noise ξ is either zero (solid lines) or $0.06V_0$ (dashed lines). The graph clearly shows that $\Delta I = I_{AB} - I_{BE}$ remains positive even for low transmission, equivalent to a 55-km propagation distance, including security margins in excess noise evaluation.

Given this raw available secret information rate, the secret bits still have to be extracted from the Gaussian data. Presently this is done using a ‘‘sliced reconciliation’’ algorithm [13], with an efficiency which is typically 0.7 to 0.8 of Shannon’s limit in our operating conditions. Eve’s information about the key is finally erased by a standard privacy

amplification procedure. These algorithms are being interfaced with the experiment. The present version of reconciliation algorithm implements true one-way reconciliation based on turbocodes [14], which eliminates the need for extra assumptions when using RRCS protocols. We point out, however, that if the efficiency of the algorithms is β (with respect to Shannon’s entropy), the key rate drops to $\Delta I_{\text{eff}} = \beta I_{AB} - I_{BE}$, and vanishes beyond approximately 20 km. Another limitation is the speed of reconciliation algorithms, which is currently able to process data at about 100 kHz, using an average PC. Work is underway to improve both the speed and the efficiency of the algorithms.

As a conclusion, the setup described in this paper is functional and ready to be tested on a field scale. The current data rate is limited by the data acquisition and processing, rather than by optical components that can go as fast as 10 GHz. The homodyne detection can be extended to 100 MHz [15] by using dedicated electronics for Alice and Bob (rather than personal computers). As a consequence, rather straightforward extensions of this setup should yield up to 100 Mbit/s raw key rate in a low-loss line. The ultimate usable secret key rate will depend on further progress in data reconciliation softwares [16].

We would like to thank André Villing, who made the homodyne detection electronics. We acknowledge financial support from the European Commission through the IST-SECOQC Integrated Project.

-
- [1] F. Grosshans and P. Grangier, *Phys. Rev. Lett.* **88**, 057902 (2002).
- [2] F. Grosshans, G. Van Assche, J. Wenger, R. Brouri, N. Cerf, and P. Grangier, *Nature (London)* **421**, 238 (2003).
- [3] F. Grosshans, N. Cerf, J. Wenger, R. Tualle-Brouri, and P. Grangier, *Quantum Inf. Comput.* **3**, 535 (2003).
- [4] Frédéric Grosshans and Nicolas J. Cerf, *Phys. Rev. Lett.* **92**, 047905 (2004).
- [5] Frédéric Grosshans, *Phys. Rev. Lett.* **94**, 020504 (2005).
- [6] Miguel Navascués and Antonio Acín, *Phys. Rev. Lett.* **94**, 020505 (2005).
- [7] G. Brassard, N. Lütkenhaus, T. Mor, and B. C. Sanders, *Phys. Rev. Lett.* **85**, 1330 (2000).
- [8] Ryo Namiki and Takuya Hirano, *Phys. Rev. Lett.* **92**, 117901 (2004).
- [9] Ryo Namiki and Takuya Hirano, *Phys. Rev. A* **72**, 024301 (2005).
- [10] S. Lorenz, N. Korolkova, and G. Leuchs, *Appl. Phys. B: Lasers Opt.* **79**, 273 (2004).
- [11] A. M. Lance, T. Symul, V. Sharma, C. Weedbrook, T. C. Ralph, and P. K. Lam, *Phys. Rev. Lett.* **95**, 180503 (2005).
- [12] H. Hansen, T. Aichele, C. Hettich, P. Lodahl, A. I. Lvovsky, J. Mlynek, and S. Schiller, *Opt. Lett.* **26**, 1430 (2001).
- [13] G. Van Assche, J. Cardinal, and N. Cerf, *IEEE Trans. Inf. Theory* **50**, 394 (2004).
- [14] Kim-Chi Nguyen, Gilles Van Assche, and Nicolas J. Cerf, *Proceedings of the International Symposium on Information Theory and its Applications, ISITA2004, Parma, Italy, 2004* (unpublished).
- [15] A. Zavatta, M. Bellini, P. Luigi Ramazza, F. Marin, and F. Tito Arecchi, *J. Opt. Soc. Am. B* **19**, 1189 (2002).
- [16] Matthieu Bloch, Andrew Thangaraj, and Steven W. McLaughlin, e-print cs.IT/0509041.